PERGAMON

Chemical Engineering Science 54 (1999) 5145–5152

Chemical Engineering Science

Counter-current operation of a structured catalytically packed-bed reactor: Liquid phase mixing and mass transfer

A.P. Higler[a,b], R. Krishna[a,*], J. Ellenberger[a], R. Taylor[b]

[a]*Department of Chemical Engineering, University of Amsterdam, Nieuwe Achtergracht 166, NL-1018 WV Amsterdam, Netherlands*
[b]*Department of Chemical Engineering, Clarkson University, Potsdam, NY 13699-5705, USA*

Abstract

The liquid-phase residence time distribution has been measured in two structured packed column configurations, of 0.1 and 0.24 m diameter, in which the catalyst particles are enclosed within wire gauze envelopes ("sandwiches"). In order to interpret these results Computational Fluid Dynamics (CFD) has been used to model the liquid flow within the packed sandwich structures. A representative sandwich structure, containing catalyst particles, is modeled as a set of triangular tubes ("Toblerones"), intersecting at 90° angles. The liquid flowing in a tube has the possibility of maintaining its flow direction or taking a sharp 90° turn. Using CFD, the dispersion characteristics of the "cross-over" junction can be determined as a sum of two components: straight-through and 90°-turn flow. The dispersion characteristics of the entire sandwich can be estimated reasonably well from information on the number of cross-over junctions along the flow direction. Comparison of the liquid-phase RTD measured in the two columns with those determined from CFD lead to the conclusion that there is channeling of liquid through the open channels, with good interchange of liquid between the open and packed channels. Liquid-phase mass transfer within the packed channels is studied also by means of CFD techniques. Due to the "upheaval" caused by the flow splitting at the crossovers, the mass transfer coefficient is about 2–3 times larger than for fully developed laminar flow in a circular tube.

Keywords: Structured packings; Counter-current flow; Liquid backmixing; Computational fluid dynamics; Mass transfer

1. Introduction

There is considerable academic and industrial interest in the area of reactive (catalytic) distillation. The catalyst particle sizes used in such operations are usually in the 1–3 mm range. Counter-current operation of gas and liquid phases in fixed beds packed with such particles is difficult because of flooding limitations. To overcome the limitations of flooding the catalyst particles have to be enveloped in wire gauze packing. The gas phase will flow preferentially in the open channels between the wire gauze envelopes. Xu, Zhao and Tian (1997) have studied the hydrodynamics of a column consisting of cylindrical catalyst "bundles". Bart and Landschützer (1996) have used the KATAPAK-S configuration of Sulzer for carrying out the process for making propyl acetate by reactive distillation. The KATAPAK-S structure is shown schematically in Fig. 1. There are several anticipated advantages of the KATAPAK-S configuration over the cylindrical bundles used by Xu et al. (1997). Firstly, there is no possibility of gas channeling in the KATAPAK-S configuration. Secondly, the catalyst envelopes in the KATAPAK-S structure consist of wire gauze structures, which are corrugated, and these corrugations cross each other at 90° angles. The effect of this is to ensure that the liquid flowing inside the catalyst envelopes or "sandwiches" is forced to change directions frequently, ensuring good radial distribution of both gas and liquid phases. For reactor design and scale up purposes, it is essential to have the information on the gas–liquid-phase residence time distributions (RTD) and interphase mass transfer; such information is lacking in the published literature.

The hydrodynamics of gas and liquid phases within the KATAPAK-S structure is quite complex. We would normally expect the gas phase to flow upwards through the

* Corresponding author. Tel.: + 31-20-525-7007; fax: + 31-20-525-5604.
E-mail address: krishna@chemeng.chem.uva.nl (R. Krishna)

0009-2509/99/$ - see front matter
PII: S0009-2509(99)00229-8

"open" channels. The downflowing liquid phase must be made to come into intimate contact with the catalyst particles and should therefore flow predominantly through the packed "sandwich" channels. There is, however, an additional requirement that the mass transfer between the gas and liquid phases should be adequately high. Under the "ideal" flow conditions described above, the interface between the gas and liquid phases will be equal to the external surface area of the packed channels. The mechanism of mass transfer in the liquid phase will be convective diffusion of the transferring species within the sandwich structures.

The objectives of the present study is to obtain some insights into the complex gas–liquid hydrodynamics in the KATAPAK-S structures, concentrating our attention on the liquid phase flow and RTD and liquid-phase mass transfer. We adopt two different approaches to obtain the required insights. First, the "ideal" flow situation sketched above, in which the liquid phase flows only within the sandwich structures, is modeled using Computational Fluid Dynamics (CFD), to obtain information on the liquid phase dispersion and mass transfer. Second, we performed experiments for liquid holdup and RTD with two different KATAPAK-S geometries (details in Table 1). A combination of CFD and experimental data is used to obtain an understanding of the hydrodynamics.

2. Experimental

The experiments have been performed with two types of structured packing elements of similar geometry but different hydraulic diameters of the open channels of 7 and 20 mm, respectively. These two packing configurations are housed in columns of 0.1 and 0.24 m diameters, see Fig. 1. Geometric details of the two configurations are listed in Table 1. Counter-current operation with the system air–water was studied. The "catalyst" particles used inside the sandwiches consisted of 1 mm glass spheres.

In Fig. 2 a schematic view of the experimental set-up of the counter-current gas–liquid reactor ($D_T = 0.10$ m)

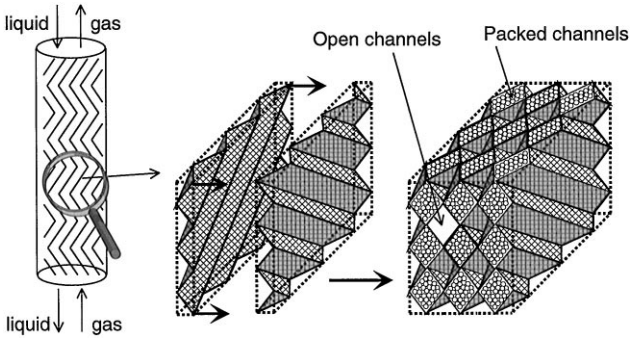

Fig. 1. Schematic of structured packing with catalyst particles inside envelopes or "sandwiches".

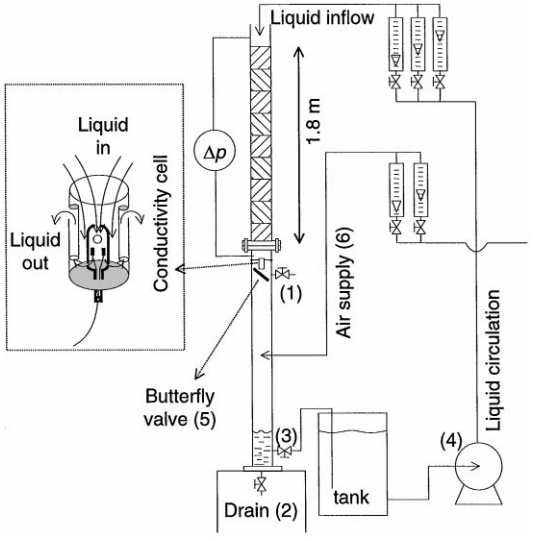

Fig. 2. Schematic diagram of the experimental set-up. The inset shows the conductivity cell used for liquid-phase RTD measurements.

Table 1
Characteristic parameters of the 0.10 and 0.24 M diameter catalytically structured packed columns

	$D_T = 0.1$ m	$D_T = 0.24$ m
Number of packed sections used in the column	9	6
Height of the reactor, m	1.8	1.705
Total mass of solids in reactor, kg	9.1687	44.020
Void fraction within "packed channels",	0.37	0.37
Volume fraction of "packed channels" in reactor, ε_{PC}	0.375	0.400
Volume fraction of "open" channels, ε_{OC}	0.625	0.600
Static liquid holdup in reactor	0.0282	0.0161
Specific surface A_{sp} for the gas flow assuming the space between the glass spheres is completely filled with liquid, m^{-1}	354.4	122.3
Hydraulic diameter of the open channels d_h, mm	7	20
Inclination of the corrugated sheets, α	45°	45°

with structured packing is shown. The liquid phase is pumped from a temperature-controlled reservoir to the top of the column by means of a centrifugal pump (Allweiler Italia, Type NB40·160·155). The recirculated liquid flow is controlled by one of the three carefully calibrated rotameters of different ranges. The maximum superficial liquid velocity is restricted to $U_L = 0.05$ m/s for the reactor with $D_T = 0.1$ m and $U_L = 0.02$ m/s for the reactor with $D_T = 0.24$ m. Using another set of two calibrated rotameters of different ranges, a known gas flow can be fed to the bottom of the column. The gas leaves at the top of the column at atmospheric condition. The total height of the column is 4 m, the upper part of which is packed with the KATAPAK-S elements. The temperature of the liquid reservoir is maintained constant (equal to the gas temperature) by a large copper cooling tube connected to a Haake F3 temperature control unit.

When steady-state conditions have been established, the dynamic liquid holdup is measured by stopping the gas and liquid supply and closing the butterfly valve (5) simultaneously. Then the liquid in the bottom section of the column is drained. By opening the valves (5) and (2), the liquid in the upper part of the reactor is collected during half an hour. From the collected liquid mass, the dynamic liquid holdup can be calculated. Measurements of the liquid-phase residence-time-distribution (RTD) have been performed by injecting a tracer pulse (saturated NaCl-solution) at the top of the reactor and registration of the salt concentration as a function of time at the bottom of the reactor. The tracer injection system as well as the conductivity cell for the tracer response measurements is positioned at the centerline of the reactor. A schematic view of the conductivity cell device is shown in the inset to Fig. 2. In a companion paper (Ellenberger & Krishna, 1999) we have reported experimental data on the gas-phase pressure drop and liquid holdup. Further details of our experimental set up and measurement techniques are available on our web site: http://ct-cr4.chem.uva.nl/strucexpts.

3. Liquid-phase RTD experimental results

By injecting salt tracer in the inflowing liquid phase and monitoring the concentration at the bottom of the column the liquid-phase residence time distributions were determined at various superficial liquid velocities U_L and at three different superficial gas velocities U_G. There was no significant influence of the superficial gas velocity on the residence time distribution. Typical RTD curves for $U_G = 0.3$ m/s and for various values of U_L for the two column configurations are shown in Fig. 3.

The axial dispersion coefficient of the liquid phase $D_{ax,L}$ can be determined by fitting the measured response to

$$E(t/\tau) = \frac{1}{2\sqrt{\pi t/\tau Pe}} \exp[-(1 - t/\tau)^2/(\pi t/\tau Pe)], \quad (1)$$

where the Peclet number, Pe, and average liquid-phase residence time τ are defined by

$$Pe \equiv \frac{U_L L}{\varepsilon_L D_{ax,L}}; \quad \tau \equiv \frac{L}{(U_L/\varepsilon_L)}. \quad (2)$$

The values of the axial dispersion coefficient $D_{ax,L}$ are presented in Fig. 4 as a function of the liquid-phase Reynolds number, $Re_{L,h}$, defined in terms of the hydraulic diameter $d_h = 4$ (volume of structure)/(wetted area), and

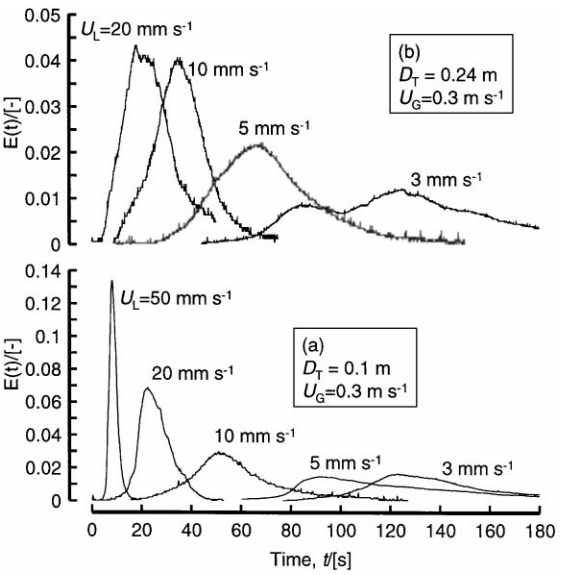

Fig. 3. Liquid residence time distribution for the (a) 0.1 m and (b) 0.24 m diameter columns measured at various superficial liquid velocities.

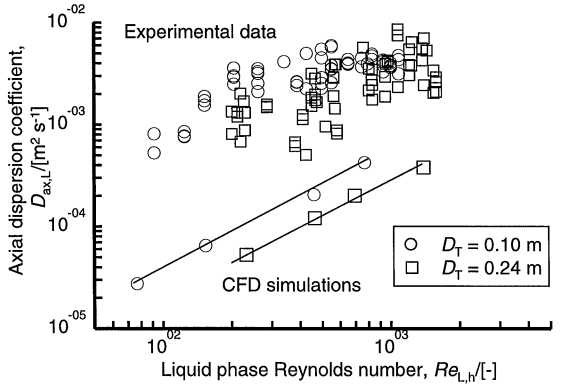

Fig. 4. Liquid-phase axial dispersion coefficient for structured packed columns. Comparison of experimental measurements with that determined from CFD simulations of liquid flow within the sandwich structures.

the absolute velocity of the liquid (U_L/ε_L). The measured liquid holdups were used in the calculation of the Reynolds number. We note that the values of the axial dispersion coefficient $D_{ax,L}$ are practically independent of the column diameter and depend only on $Re_{L,h}$.

In order to interpret the measured liquid RTD results, we resort below to CFD techniques.

4. CFD simulations of liquid-phase RTD in packed channels

In the "ideal" flow situation the liquid flows downward through the packed channels and the gas flows upward through the open channels. The "ideal" flow situation for the liquid phase can be modeled using CFD techniques. We focus on flow inside two representative sandwich geometries, small and large, which correspond to column diameters of 0.1 and 0.24 m (Fig. 5). Each sandwich structure is considered to be made up a series of intersecting tubes of triangular cross-section, which we popularly refer to as Toblerone (yes, Swiss chocolate!) structures. The gas flow in the "open" channels is not considered in the CFD analysis. We also aim to derive the flow characteristics of an entire column using the knowledge of the flow characteristics of one crossover.

Liquid can only enter the sandwich structure through the top and only leave through the exits in the bottom of the sandwich. The faces of the sandwich, which in practice are formed by the metal gauze are modeled to be impermeable walls. Inside the sandwich structure we have two phases, the liquid and the catalyst particles. In the simulations the particles are taken to be uniform spheres of 1 mm diameter (corresponding to our experiments). The liquid flow field is obtained by solving the equations of continuity of mass

$$\frac{\delta}{\delta t}(\rho_L v_L) + \nabla(\varepsilon_L \rho_L \boldsymbol{v}_L) = 0 \tag{3}$$

along with the Navier–Stokes equations

$$\frac{\delta \rho_L v_L}{\delta t} + \nabla\bullet(\rho_L \boldsymbol{v}_L \boldsymbol{v}_L - \mu_L(\nabla \boldsymbol{v}_L + (\nabla \boldsymbol{v}_L)^{\mathrm{T}})) = \boldsymbol{B} - \nabla p. \tag{4}$$

A commercial CFD package CFX 4.1c of AEA Technology, Harwell, UK, was used to solve the equations of continuity and momentum. This package is a finite volume solver, using body-fitted grids. The grid geometry used is shown in Fig. 5. The grids are non-staggered and all variables are evaluated at the cell centers. An improved version of the Rhie-Chow (1983) algorithm is used to calculate the velocity at the cell faces. The pressure–velocity coupling is obtained using the SIMPLEC algorithm (Van Doormal & Raithby, 1984). For the convective terms in Eqs. (3) and (4) hybrid differencing was used. A fully implicit backward differencing scheme was used for the time integration.

In order to consider the influence of the catalyst particles inside the sandwich structures, the porous medium option of CFX 4.1c is invoked. In this option a constant void fraction, $\varepsilon = 0.37$, inside the sandwiches is assumed and the influence of the solids phase is accounted for by specification of an extra body force **B** in the Navier–Stokes equations (cf. Eq. (4)) which is the extra pressure drop, calculated by the Ergun equation

$$\mathbf{B} = 150\frac{\mu_L \boldsymbol{v}_L}{d_p^2}\frac{(1-\varepsilon)^2}{\varepsilon^2} + \frac{1.75\rho_L \boldsymbol{v}_L^2}{d_p}\frac{(1-\varepsilon)}{\varepsilon}. \tag{5}$$

This method of using the Ergun equation for describing flow in porous media has adopted by Parsons and Porter (1992) to study gas flow patterns in packed beds, by Hayes, Afacan, Boulanger and Shenoy (1996) to study flow in pores, and by Van Gulijk (1998) to study transversal dispersion in structured packed beds.

Three types of simulations were performed

(1) Residence time distribution studies in intersecting Toblerone structures of two geometries (small and large) with dimensions as shown in Fig. 5.
(2) Residence time distribution in two sandwich structures of 0.1 and 0.24 m width as shown in Fig. 5. These sandwich structures were made up of Toblerones of varying lengths.
(3) Residence time distribution in a single triangular tube.

In all the three cases above, the walls were modeled as solid boundaries and the no-slip boundary condition was invoked. At the outlet, a free outflow boundary condition was specified and constant pressure was maintained. After sufficient time to allow steady-state to be reached, a pulse of tracer (a second component in the liquid phase with otherwise identical properties as the liquid) was

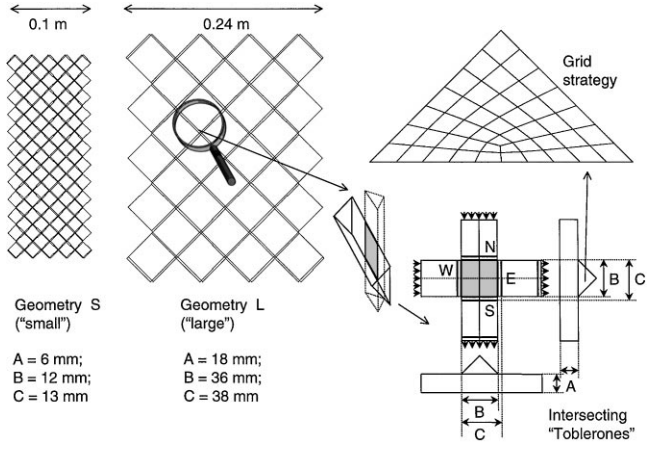

Fig. 5. Geometry of small and large sandwich structures used in CFD simulations.

injected uniformly at the inlet and the compositions monitored at a station, either the outlet or at a specified face of the structure. Since the physical properties of the fluid and the tracer are identical, the flow fields of the fluid will not be influenced by the tracer. This method has been used successful by Togatorop, Mann and Schofield (1994) to study mixing in a stirred tank. Further details of the simulations, including animations, have been placed on our web site: http://ct-cr4.chem.uva.nl/strucpack.

The residence time distribution data obtained with the CFD calculations was analyzed by means of an axial dispersion model with the exit age distribution given by Eq. (1) with a variance

$$\sigma^2 = \tau^2\left(\frac{2}{Pe} - \frac{2}{Pe^2}(1 - \exp(-Pe))\right). \quad (6)$$

From the RTD data the mean residence time τ, the Peclet number, Pe, and the axial dispersion coefficient $D_{ax,L}$ can be determined.

4.1. RTD of single cross-over

Consider flow in a single crossover with the liquid flowing into the north and west faces and leaving at the east and south faces. Tracer was injected at the north plane N just before the junction, as indicated in Fig. 5, and monitored at the east (E) and south (S) faces. The RTD studies showed that flow-splitting between the E and S faces is roughly equal with a slight preference for the east channel; see Fig. 6. This preferential flow is due to the fact that the triangular geometry is a right triangle and not an equilateral triangle (the latter is expected to split the flow equally).

The exit age distributions of the straight-through (south face) and 90°-turn (east face) flows are shown in Fig. 7 for a typical simulation. These $E(t)$ curves can be fitted to the axial dispersion model to obtain $D_{ax,L}$; the results are shown in Fig. 8. As expected, there is a higher dispersion for the flow that takes a 90° turn. It is also interesting to note that the dispersion characteristics of the straight-through flow is only slightly higher than of a single triangular tube without cross-over. This is because the "straight-through" flow has to displace upwards to get into the intersecting Toblerone, increasing the mean residence time and dispersion.

4.2. RTD of packed sandwich structures

For the small (0.1 m) and large (0.24 m) sandwich structures, with 12 and 5 crossovers in the liquid flow direction, tracer studies were carried out to determine the RTD of the entire sandwich. The exit age distributions for a range of liquid velocities through the packed channels, $U_{L,pack}$, are shown in Fig. 9 for the two sandwich configurations. When comparing these CFD simulation

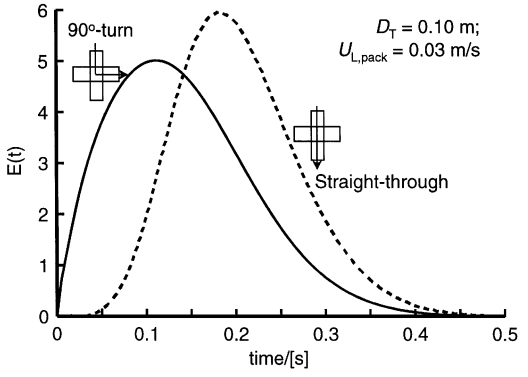

Fig. 7. Exit age distributions at the south face (straight-through flow) and at the east face (90°-turn) for tracer injection at the north face for single cross-over.

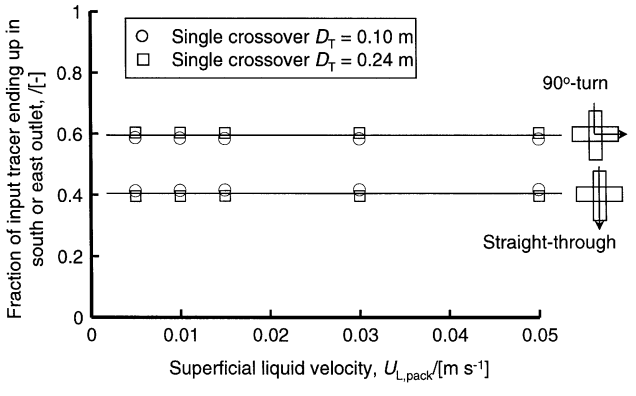

Fig. 6. Fraction of tracer flowing either straight-through or taking a 90°-turn for single cross-over.

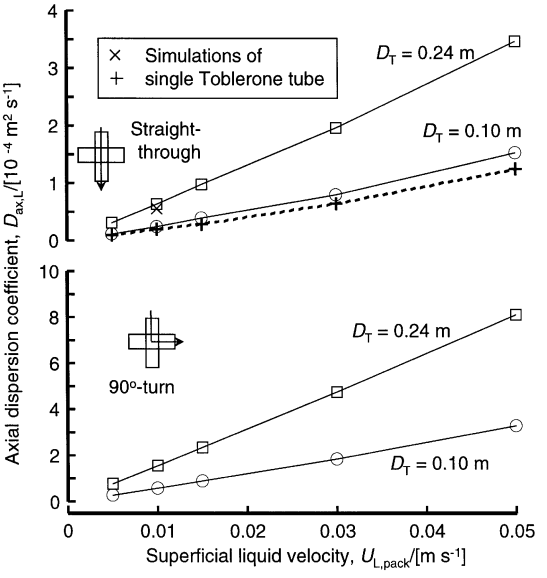

Fig. 8. Axial dispersion coefficients for single cross-over.

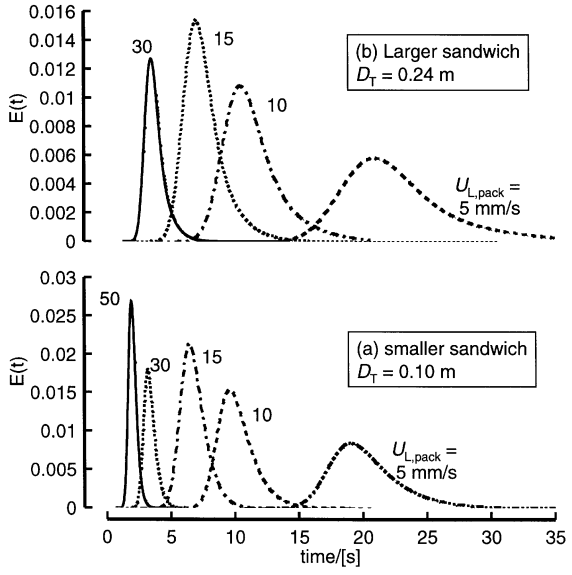

Fig. 9. Exit age distributions for (a) 0.1 m and (b) 0.24 m diameter sandwich structures for a variety of liquid velocities through the packed section.

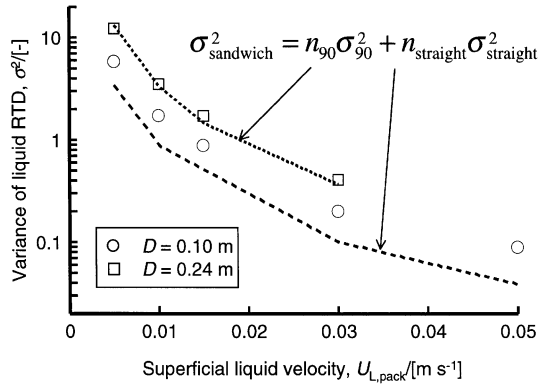

Fig. 10. Variance of the liquid-phase RTD for small and large sandwich structures shown in Fig. 7. Comparison with predictions from Eq. (7).

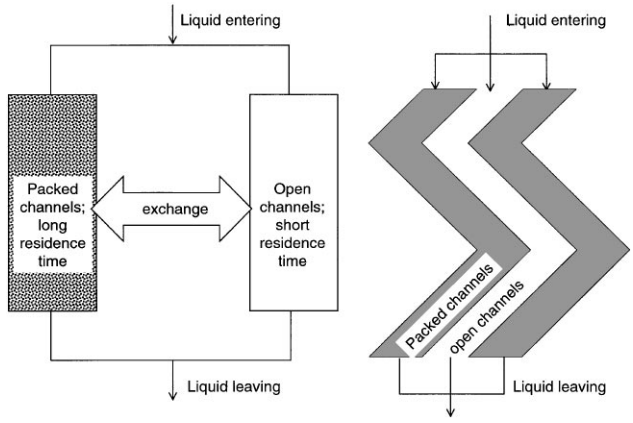

Fig. 11. Schematic of liquid flow in structured packed column.

results with the experimental measurements (Fig. 3) it must be borne in mind that the superficial velocity through the sandwich structures, $U_{L,\mathrm{pack}} = U_L/\varepsilon_{PC}$. The mean residence times obtained from CFD are systematically less than the ones obtained from a material balance; this is due to small dead zones at the walls of the sandwiches. These wall effects are more predominant for the smaller sandwich structure of 0.1 m diameter. This is due to the fact that there are more "dead end zones" at the walls per meter of packing length. The variance of the RTD for the two sandwich structures is shown in Fig. 10. Also shown in Fig. 10 are calculations of the variance based on the number of crossovers experienced in the flow path

$$\sigma^2_{\mathrm{sandwich}} = n_{90}\sigma^2_{90} + n_{\mathrm{straight}}\sigma^2_{\mathrm{straight}}\,. \qquad (7)$$

The predictions of Eq. (7) for the large sandwich are seen to be very good while the agreement for the smaller sandwich of 0.1 m is less good because of excessive wall effects for small diameter columns. We conclude that the liquid-phase RTD inside large-scale sandwich structures can be estimated reasonably accurately on the basis of the characteristics of a single crossover. This is a useful scale up strategy.

The axial dispersion coefficients for the small and large structures, determined from CFD simulations are found to be about a factor 50 lower than those measured experimentally; see Fig. 4. The much higher values of the liquid-phase dispersion obtained in the experimental measurements points to a high degree of bypassing of the liquid through the open channels. We envisage the liquid flowing downwards splitting into two portions, one portion flows through the packed channels and the other portion flows through the open channels; see Fig. 11.

The measured liquid-phase RTD is the same irrespective of whether the tracer is injected in the packed channels or in the open channels. This can be evidenced by the RTD measurements shown in Fig. 12 for the 0.24 m diameter column. This implies that there is a very good exchange between the liquid in the open and packed channels; see Fig. 11. From a reactor engineering standpoint, this is good news because the liquid flowing in the packed channels is in intimate contact with the catalyst whereas the liquid in the open channels does not "see" the catalyst phase. However, because there is excellent interchange between the liquid phases present in the open channels and packed channels, the contacting efficiency of the liquid is perhaps not impaired due to bypassing of the liquid flowing through the open channels.

The axial dispersion coefficients $D_{\mathrm{ax},L}$ for the structured packed columns are roughly about one order of magnitude higher than the corresponding values for trickle-bed operation (Ellenberger & Krishna, 1999; Sie & Krishna, 1998). This is to be expected because of the

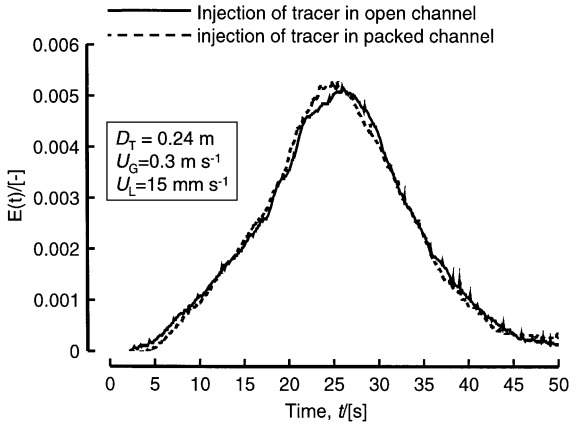

Fig. 12. Liquid residence time distribution for the 0.24 m diameter column measured measured with two different tracer injection strategies: (a) tracer injection in the packed section and (b) tracer injection in the liquid in the open channels.

bypassing of the liquid through the open channels. Such large-scale bypassing is not possible in conventional trickle-bed operation. The high axial dispersion coefficients for the liquid phase in structured packed columns is not of great consequence for commercial columns with heights exceeding say 3 m; in such cases plug flow of the liquid phase is assured. However, for short laboratory reactors shorter than say 0.5 m in height would suffer from backmixing of the liquid and this would need to be taken into account when interpreting reaction kinetics data (Bart & Landschützer, 1996).

5. Liquid phase mass transfer in sandwich structures

We use CFD techniques for determining the liquid-phase mass transfer coefficient within the two sandwich structures shown in Fig. 5. The flow is first allowed to stabilize and then a tracer component is introduced through the walls of the structure by maintaining the mass fraction of the tracer at the wall to be unity. By monitoring the tracer concentration in the outflowing liquid as a function of time, we can determine the mass transfer coefficient from a tracer material balance during the monitoring period. The Sherwood number, defined in terms of the hydraulic diameter of the packed channels, d_h, is

$$Sh = k_L d_h / \mathcal{D}, \tag{8}$$

where $\mathcal{D}$ is the diffusion coefficient of the tracer in water, taken to be 1×10^{-9} m^2/s in the simulations. The Sherwood number defined in this way is found to be the same for both small and large structures and independent of the Reynolds number. Mass transfer within the sandwich structures is dominated by the mixing process at the frequent crossovers; the flow velocity is not the determining factor. The Sherwood number is about a factor 2.5

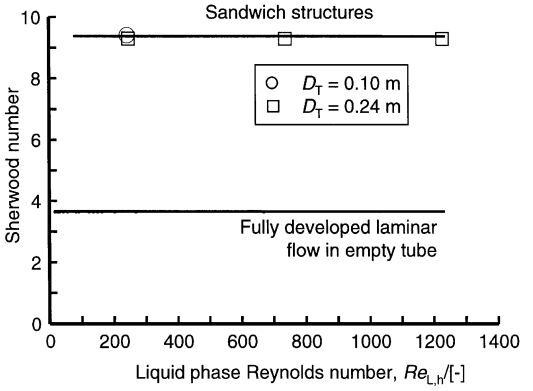

Fig. 13. Liquid-phase mass transfer within sandwich structures. The Sherwood number is plotted as a function of the liquid-phase Reynolds number, both defined in terms of the hydraulic diameter.

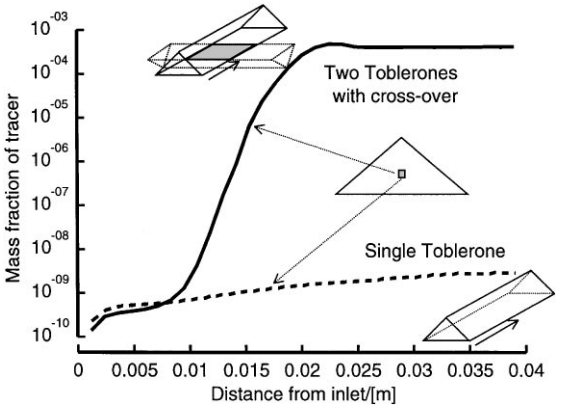

Fig. 14. Mass fraction of tracer at the center of a Toblerone as a function of the distance from the inlet.

higher than for laminar flow inside a circular tube; see Fig. 13. In order to understand this higher value of the Sherwood number we also carried out simulations of the mass transfer in a single Toblerone tube and two Toblerones which cross each other at right angles. After steady-state flow has been established, wall tracer is introduced and maintained at the walls. Fig. 14 shows the mass fraction of the tracer monitored at the center of a tube. The effectiveness of the cross-over junction is evidenced by the fact that the tracer concentration at the monitoring point experiences a sharp increase at the position of the junction. The cross-over junction causes an upheaval and mixes up the liquid phase very effectively. The simulation of a single Toblerone tube is in sharp contrast to the above and the tracer concentration maintains a low, almost constant value.

6. Concluding remarks

CFD studies of liquid flow through packed structures show that the RTD of the liquid phase can be estimated

reasonably accurately based on the RTD characteristics of a single cross-over. This is a useful result because it allows the determination of the RTD behaviour of large structures on the basis of CFD studies on a single cross-over.

A combination of the CFD simulation results with measurements of the liquid-phase RTD for counter-current gas–liquid flow in a structured packed reactor show that there is considerable channeling of the liquid phase through the open channels; see Fig. 11. Further experimental work is required to determine the efficiency of liquid exchange between the packed and open channels.

Mass transfer within the sandwich structures is dominated by the mixing experienced at the cross-overs and is practically independent of the liquid flow velocity. This is a useful result for design and scale up.

Notation

A_{sp}	specific surface of "open" channels, 1/m
$\mathbf{B}$	body force, N/m^3
d_h	hydraulic diameter, m
d_p	particle diameter, m
$Đ$	liquid-phase diffusion coefficient, m^2/s
$D_{ax,L}$	axial dispersion coefficient, m^2/s
D_T	diameter of reactor, m
E	exit age distribution function, dimensionless
g	acceleration of gravity, 9.81 m/s^2
k_L	mass transfer coefficient, m/s
L	length of reactor, m
n	number of cross-overs, dimensionless
p	pressure, Pa
Pe	Péclet number, dimensionless
$Re_{L,h}$	Reynolds number $\rho_L(U_L/\varepsilon_L)d_h/\mu_L$, dimensionless
Sh	Sherwood number, dimensionless
t	time, s
U_G	superficial gas velocity in the column, m/s
U_L	superficial liquid velocity in the column, m/s
$U_{L,pack}$	superficial liquid velocity through packed "sandwich", $U_{L,pack} = U_L/\varepsilon_{PC}$, m/s
v_L	absolute liquid velocity inside the packed structures, m/s

Greek letters

ε	holdup, dimensionless
μ	viscosity, Pa s
ρ	density, kg/m^3
σ	surface tension, N/m
τ	mean residence time, s

Subscripts

h	hydraulic
s	solid phase
G	gas phase
L	liquid phase
OC	open channel
PC	packed channel
T	tower or column

Acknowledgements

The KATAPAK-S elements used in this work were made available to us by Sulzer Chemtech Ltd., Switzerland.

References

Bart, H. -J., & Landschützer, H. (1996). Heterogene Reaktivdestillation mit axialer Rückvermischung. *Chemie Ingenieur Technik*, *68*, 944–946.

Ellenberger, J., Krishna, R., (1999). Counter-current operation of structured catalytically packed distillation columns: pressure drop, holdup and mixing. *Chemical Engineering Science*, *54*, 1339–1345.

Hayes, R. E., Afacan, A., Boulanger, B., & Shenoy, A. V. (1996). Modeling the flow of power law fluids in a packed bed using a volume averaged equation of motion. *Transport in porous media*, *23*, 175–196.

Parsons, I. M., & Porter, K. E. (1992). Gas flow patterns in packed beds: a computational fluid dynamics model for wholly packed domains. *Gas Separation and Purification*, *6*, 221–227.

Rhie, C. M., & Chow, W. L. (1983). Numerical study of the turbulent flow past an airfoil with trailing edge separation. *AIAA Journal*, *21*, 1525–1532.

Sie, S. T., & Krishna, R. (1998). Process Development and Scale Up: III. Scale up and scale down of trickle-bed processes. *Reviews in Chemical Engineering*, *14*, 203–252.

Togatorop, A., Mann, R., & Schofield, D. F. (1994). An application of CFD to inert and reactive tracer mixing in a batch stirred vessel. *A.I.Ch.E. Symposium Series No. 299,* , *90*, 19–32.

Van Doormal, J., & Raithby, G. D. (1984). Enhancement of the SIMPLE method for predicting incompressible flows. *Numerical Heat Transfer*, *7*, 147–163.

Van Gulijk, C. (1998). Using computational fluid dynamics to calculate transversal dispersion in a structured packed bed. *Computers and Chemical Engineering*, *22*, S767–S770.

Xu, X., Zhao, Z., & Tian, S. J. (1997). Study on catalytic distillation processes, Part III. Prediction of pressure drop and holdup in catalyst bed. *Transactions of the Institution of Chemical Engineers Part A* , *75*, 625–629.